

A Dual Band CRLH Metamaterial-Inspired Planar Antenna for Wireless Applications

Junuthula ASHISH, Amara PRAKASA RAO

Dept. of ECE, National Institute of Technology, Warangal, 506004, Telangana, India

jashrddy@gmail.com, aprao@nitw.ac.in

Submitted November 15, 2021 / Accepted February 22, 2022

Abstract. *This paper presents the design of a metamaterial based dual band dual-polarized monopole antenna applicable for wireless applications. A monopole antenna is designed and loaded with a CRLH MTM inspired unit cell on either side of the substrate to operate as a dual band antenna with an improved impedance matching and circular polarization in one of the bands. The overall size of the antenna is $24\text{ mm} \times 17\text{ mm} \times 1.6\text{ mm}$, operating at center frequencies of 3.5 GHz and 5.5 GHz. Measurements were carried out and the impedance bandwidths obtained in the two bands are 940 MHz (26.8%) and 490 MHz (8.9%) with linear polarization in the first band and circular polarization with an axial ratio bandwidth of 150 MHz in the second band of operation. The obtained peak gains of the antenna in the two bands are 4 dBi and 5.1 dBi respectively, with a considerable agreement between the simulated and measured results.*

Keywords

CRLH, dual band, linear polarization, circular polarization

1. Introduction

The development and use of metamaterials in the design of the antenna has widely increased in the recent years. Metamaterials (MTMs) offer unusual properties which are not present in the naturally available materials and help in realizing antennas with an improved performance on multiple facets. Some of these could be the realization of multiband, wideband, low profile and high gain antennas [1]. With an ever-evolving wireless communication technology and miniaturization of the wireless operating gadgets, the need for the antennas capable of operating in multiple bands without losing their low-profile nature [2–4] is of utmost priority. With proper loading of metamaterial cells into the design of the conventional antennas can address some of these requirements [5]. The left-handed nature of the metamaterials helps in exhibiting negative permeability and negative permittivity simultaneously, which are unusual with the existing right-handed

materials. MTMs additionally showcase antiparallel phase velocities and group velocities, negative refractive index (NRI) and zero order resonance (ZOR) modes.

Composite right left-handed (CRLH) transmission line metamaterial (TL-MTM) provide zeroth-order resonance (ZOR) modes which are useful in designing miniaturized multiband antennas. CRLH TL-MTM possess both right and left-handed effect with a series and parallel combination of capacitor and inductor providing the ZOR [6]. The ZOR frequency of the antenna is independent of its physical size and hence can be used as an advantage in miniaturization of the antenna. Several techniques have been used to realize multiband antennas like reconfigurability [7], [8] or by loading capacitive elements [9] but increase the design complexity. CRLH MTMs are suitable in realizing the multi band antennas using higher order resonances but may offer less gain due to their small size. However, high gain offering monopole antennas loaded with the CRLH cells could serve the purpose.

The traditional monopole antenna with MTM loading, introduces the second resonance in addition to the regular monopole resonance are proposed [10], [11], operating at 2.4/5/5.2/5.8 GHz WLAN and 5.5 GHz for Wi-Fi applications. Antennas loaded with CRLH unit cell to achieve dual band nature based on the ZOR for wireless applications are realized [12–15]. However, the aforementioned antennas are slightly larger in volume. In [16], a single feed dual band antenna loaded with mushroom like TL-MTM structure with circuit analysis is presented. A 2×2 array formed by the unit cell elements is loaded to the conventional microstrip patch antenna and a similar mushroom unit cell loaded antenna with dual band nature and dual modes is presented [17], yet the planar nature of the antennas is lost due to the vias that are part of the mushroom unit cells. A composite metamaterial inspired antenna based on loading of inner split and outer closed-ring resonators [18], for narrow first band and wider second operation is proposed. Similarly, for 2.4/5 GHz WLAN applications, a slot antenna with miniaturized size employing a split-ring resonator (SRR) offering circular polarization in one of the bands [19] has been published. The wideband circularly polarized antenna based on polarization conversion metasurface is presented in [20], [21] and a similar

metasurface based wide-gain-bandwidth with meta surface is reported in [22]. Several antennas based on the CRLH resonant structures aimed at multiband operation are discussed [23–26].

In this paper, a simple and miniaturized dual band monopole antenna incorporated with CRLH MTM inspired unit cell, with circular polarization in one of the bands is proposed. Initially a monopole antenna is designed to operate as a single band antenna, then with the loading of the MTM inspired unit cell enables the antenna to work as a dual band antenna operating at 3.15–4.09 GHz and 5.35–5.84 GHz. The impedance bandwidths of the antenna in two bands are 26.8% and 8.9% with the maximum peak gains of 4 dBi and 5.1 dBi, respectively. The circular polarization is achieved in the second band with good radiation efficiencies in both the bands. The circuit realization and radiation properties of the antenna are also discussed. The designed antenna is suitable and can be adapted for 3.5/5.5 GHz WiMAX and mid band 5G wireless applications.

2. Antenna Design

The design and configuration of the proposed planar microstrip fed dual band antenna with the MTM unit cell is shown in Fig. 1. The overall size of the antenna along with its dimensions is mentioned in Tab. 1. The antenna design comprises of a cost effective FR4 as substrate (permittivity of 4.4 and loss tangent value 0.02) of height 1.6 mm and an L-shaped patch fed from a microstrip line that induces resonance at a frequency of 4.3 GHz. A metamaterial unit cell is designed and loaded on either side of the FR4 substrate

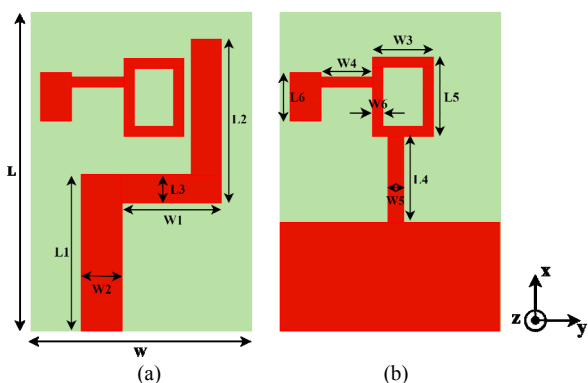


Fig. 1. Geometry and the configuration of the proposed antenna: (a) Top view and (b) bottom view.

Parameter	Value [mm]	Parameter	Value [mm]
L	24	W	17
L1	13	W1	7
L2	11.5	W2	2.5
L3	2	W3	5
L4	6	W4	4
L5	6	W5	1
L6	4	W6	0.5

Tab. 1. Optimized dimensions of the proposed antenna.

and is united with the ground on the ground side of the antenna through a thin rectangular strip. A partial ground plane is employed in the design to help in improving the bandwidth of the antenna. With the loading of the MTM unit cell, the antenna operates as a dual band resonant antenna ($S_{11} < -10$ dB) with a wider first band and the resonant frequencies 3.5 GHz and 5.5 GHz.

2.1 Design Stages of the Proposed Antenna

The evolutionary stages involved in the design of the MTM inspired antenna are depicted in Fig. 2 (a) to (d). The respective reflection coefficient and axial ratio plots of

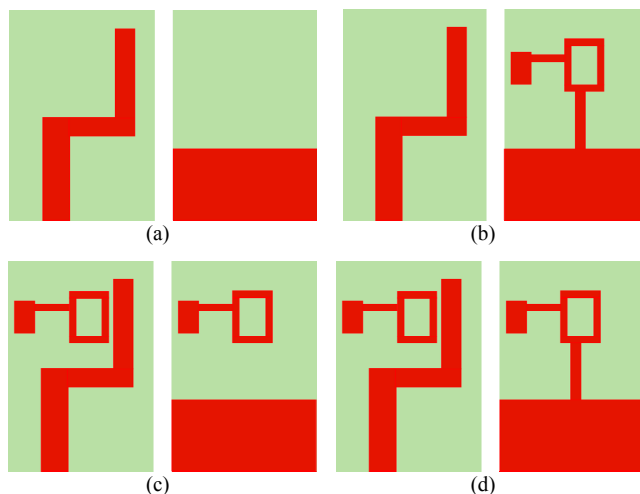


Fig. 2. Front and back view of the (a) Antenna 1, (b) Antenna 2, (c) Antenna 3 and (d) Antenna 4.

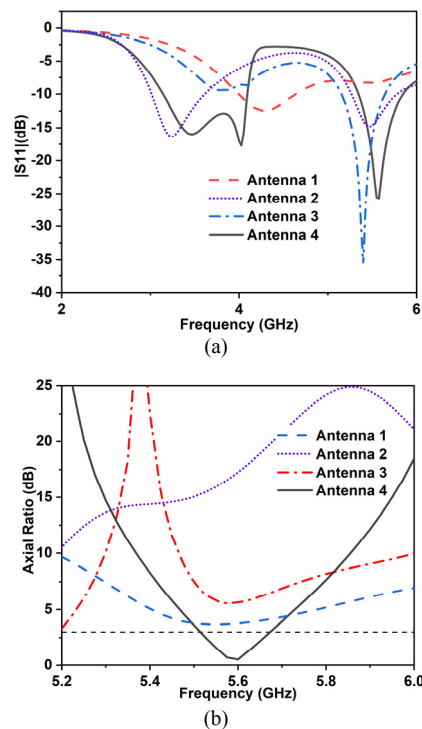


Fig. 3. Simulated design stage responses: (a) Reflection coefficient; (b) axial ratio.

the aforementioned antenna configurations are shown in Fig. 3(a) and (b). Initially an L shaped conventional patch antenna is designed and fed by a microstrip line with a partial ground plane, which resonates only in one frequency band ranging from 4–4.64 GHz with a center frequency of 4.3 GHz (as seen for Antenna 1 in Fig. 3(a)). A CRLH MTM-TL inspired unit cell is designed and is etched only on the ground side of the antenna which induces an additional band. Later unit cell is placed on either side of the substrate, inducing a resonance band near the first band along with the existing band from 5.16–5.64 GHz with center frequency of 5.4 GHz, due to the additional series and shunt elements. A thin rectangular strip is used to connect the ground with the unit cell ensuring a good impedance matching and a wider first band with a considerably large bandwidth from 3.15–4.09 GHz due to the merging of two resonances and the rectangular strip also ensures that the CP is achieved in the second band with AR < 3 dB (see Antenna 3 in Fig. 3(b)).

2.2 Circuit Realization of the Antenna

The geometry of the antenna indicates that there is a CRLH TL inspired unit cell loaded on either side of the substrate. The unit cell and its effective equivalent circuit are depicted in Fig. 4(a), and it is evident that there is a series and parallel combination of inductor and capacitor. The series capacitor C_L is provided by the gap between the L shaped radiator and the unit cell, the rectangular ring structure results in the series inductor L_R . A thin rectangular strip connected from the rectangular ring structure to the virtual ground indicated in Fig. 4(a), forms the shunt inductor L_L . The shunt capacitor C_R is provided by the solid rectangular patch etched on both the sides of the substrate. The approximate overall equivalent circuit of the proposed antenna including the main radiator and the unit cells is as shown in Fig. 4(b). In the circuit diagram, the first unit cell etched on top side of the substrate has a series

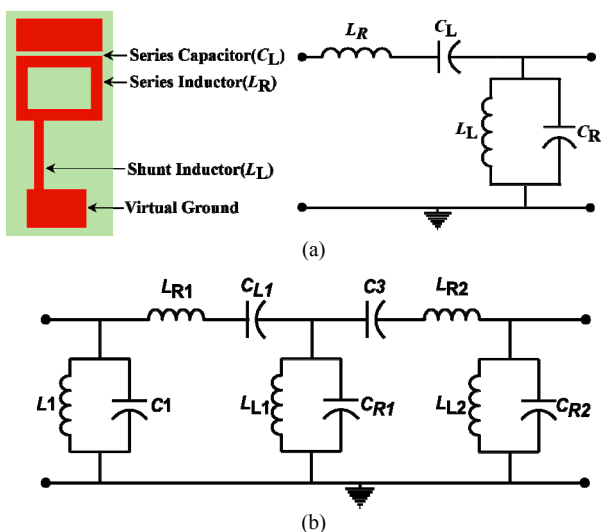


Fig. 4. Circuit realization of (a) MTM unit cell, (b) MTM loaded antenna.

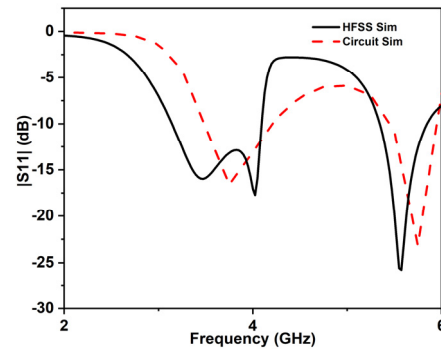


Fig. 5. Reflection coefficient responses of HFSS and circuit simulation.

arm with the elements L_{R1} , C_{L1} and shunt arm with the elements L_{L1} , C_{R1} . The cell placed on the ground side of the antenna has a series arm with inductance L_{R2} and shunt arm with inductance L_{L2} and capacitance C_{R2} . The two-unit cells are separated by the FR4 substrate acting as a dielectric and forming a capacitance C_3 . The L shaped radiator has an inductance of L_1 and a capacitance C_1 is set up by the feed line and the partial ground plane.

Further, the lumped equivalent circuit represented in Fig. 4(b) is simulated with the ADS software and the S_{11} response is compared to the HFSS simulated result. The obtained lumped element values are $L_1 = 1.775$ nH, $C_1 = 1.15$ pF, $L_{R1} = 2.675$ nH, $C_{L1} = 0.92$ pF, $L_{L1} = 1.525$ nH, $C_{R1} = 0.5$ pF, $C_3 = 0.54$ pF, $L_{R2} = 0.9$ nH, $L_{L2} = 0.69$ nH, and $C_{R2} = 1.91$ pF. A comparison is drawn between the S_{11} responses of HFSS simulation and circuit simulation results as depicted in Fig. 5 and a close match is observed between them.

3. Results and Discussions

3.1 Reflection Coefficient

The overall volume of the proposed antenna is 24 mm × 17 mm × 1.6 mm and its size in terms of λ (the free space wavelength that corresponds to the lowest resonance frequency band's center frequency) is $0.3\lambda \times 0.2\lambda \times 0.01\lambda$. Hence, the proposed antenna is of compact size with dimensions a lot less than that of the typical monopole antenna operating at the same frequency. The designed antenna has been fabricated and the prototype of the same is as shown in Fig. 6(a). The antenna's S_{11} characteristics are measured with a vector network analyzer and are illustrated in Fig. 6(b). It is observed that a decent consistency is maintained between the simulated and the measured results. It is observed from the S_{11} response of the antenna that the lower band is wider band ranging from 3.15–4.09 GHz with an impedance bandwidth of 26.8%, which is suitable for 3.5 GHz WiMAX, n77 and n78 sub-6 GHz 5G nr bands. The higher band is narrower with frequency range 5.35–5.84 GHz and an impedance bandwidth

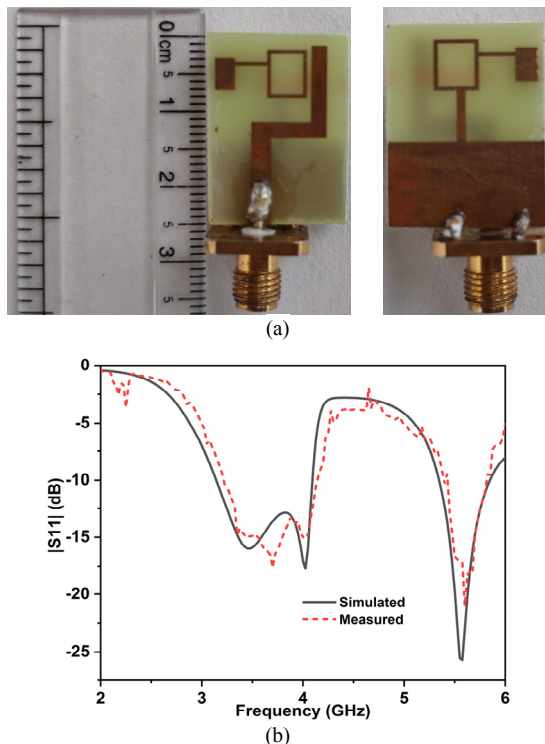


Fig. 6. (a) Front and back view of the fabricated prototype. (b) Simulated and measured reflection coefficients.

of 8.9% covering the 5.5 GHz WiMAX band. The antenna being dual band, can be well adapted in the devices having multiple applications.

3.2 Radiation Pattern

Figure 7 depicts the antenna's simulated and measured radiation patterns. A good match between the results is observed with the measured cross polarization levels slightly higher than the simulated one and the lack of smoothness in the measured results can be attributed to the losses that were incurred during the fabrication and testing of the proposed antenna. At 3.5 GHz, a monopole like radiation pattern is generated with the peak along the positive z -direction. A radiation patterns observed at 5.6 GHz frequency are slightly off due to the asymmetric feeding and the nature of the patch, the distortions are due to the antenna operating at higher order resonating modes. The more detailed representation of the radiation caused by the surface currents and the current flow of the proposed antenna are shown in Fig. 9 and Fig. 10.

3.3 Polarization

This section discusses the polarization of the designed antenna in two frequency bands. The axial ratio plot of the antenna indicates that it is below 3 dB from 5.51 to 5.66 GHz as represented in Fig. 8. The CP of the antenna is achieved from the proper loading of the MTM unit cell at the ground side and adjusting the position of the thin rectangular strip acting as an inductor. Initial L shaped monopole antenna design helps in achieving the CP at a required

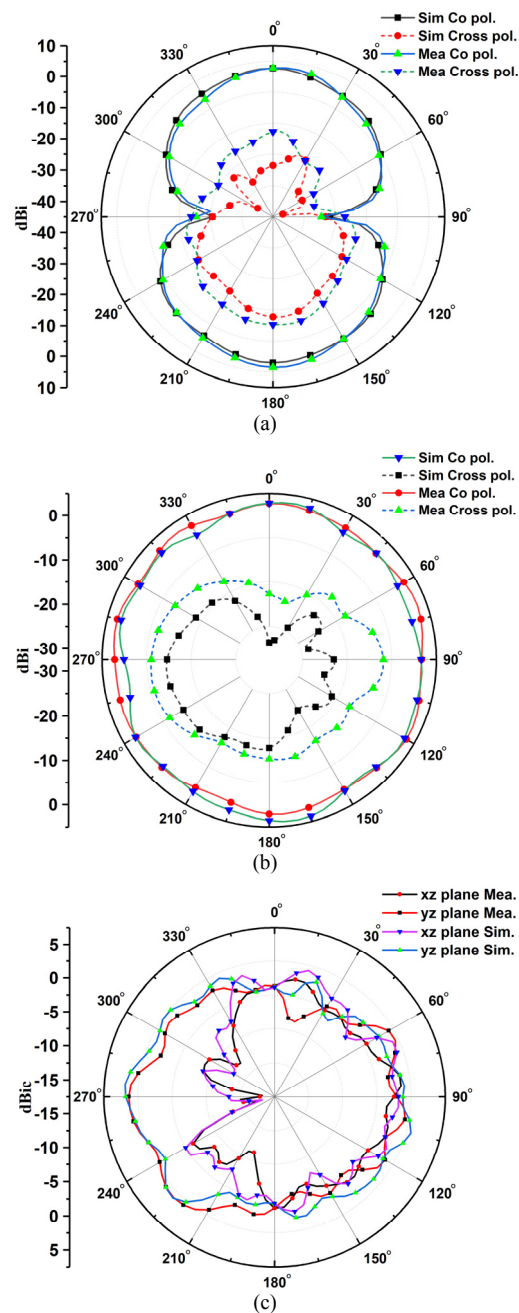


Fig. 7. The radiation patterns of the antenna in the plane: (a) XZ at 3.5 GHz, (b) YZ at 3.5 GHz, (c) XZ and YZ at 5.6 GHz.

frequency of operation. In the other band linear polarization of the antenna is observed. Hence, the antenna acts as a dual polarized antenna with linear polarization in the first band and circular polarization in the other.

The surface current distributions of the antenna are illustrated in Fig. 9. At 3.5 GHz, the strong surface currents are concentrated on the main L shaped radiator and on both the thin rectangular strips that are part of the unit cells. It is also observed that a strong current is passing through the narrow strip connected between the unit cell and the ground plane introducing an inductance. At 5.5 GHz, the strong surface currents are present at the edges of the L shaped radiator and at the strip connecting to the ground

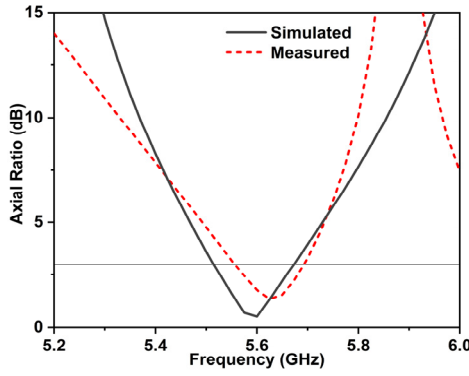


Fig. 8. Simulated and measured axial ratio responses of the antenna.

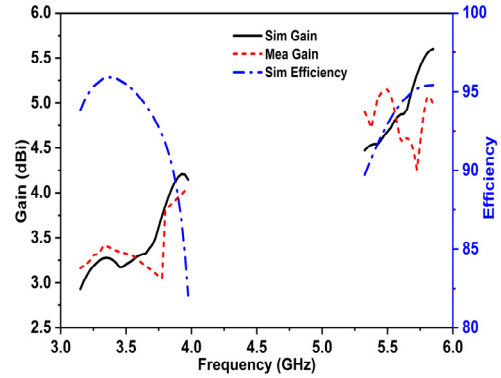


Fig. 11. Simulated, measured gains and simulated efficiency of the proposed antenna.

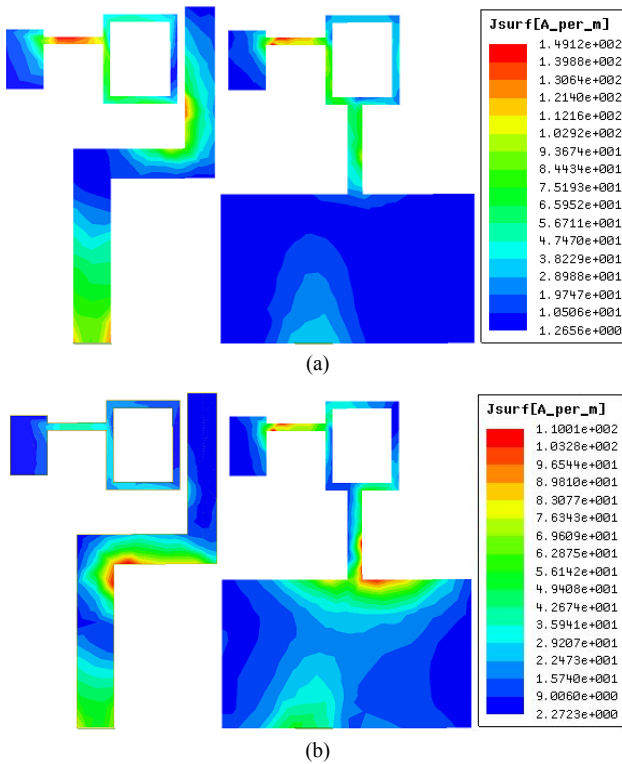


Fig. 9. Surface current distributions of the antenna at (a) 3.5 GHz and (b) 5.6 GHz.

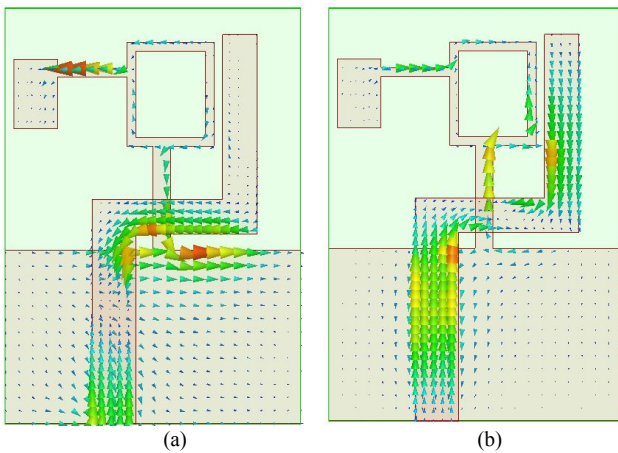


Fig. 10. Vector current distributions of the antenna at 5.5 GHz for phases (a) 0 deg and (b) 90 deg.

plane. The position of the narrow strip, part of the unit cell is adjusted to achieve the circular polarization of the antenna in the frequency band 5.51–5.66 GHz. The maximum surface current density also exists on this narrow strip representing the current flow through it and hence creating an inductance. It is also observed from Fig. 10 that the orthogonal currents with almost an equal magnitude flowing in the opposite direction through the L shaped radiator with a phase shift of 90 degrees are responsible in achieving the circular polarization.

3.4 Gain and Radiation Efficiency

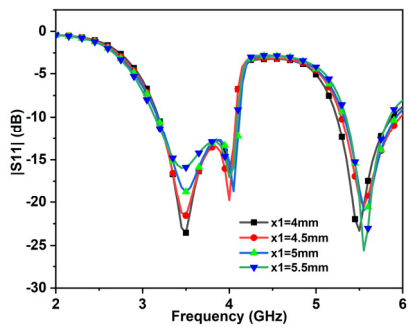
The antenna's simulated and measured peak gains in the two resonant frequency bands with center frequencies of 3.5 GHz and 5.5 GHz are shown in Fig. 11. The maximum gain that is observed within the first band is 4 dBi and in the second band is 5.2 dBi respectively. It is also noticed from the radiation efficiency plot of Fig. 11 that it is >85% in the first band and >90% in the second band. Hence, the antenna offers decent gains and good efficiencies throughout the bands of operation, making it suitable for targeted applications.

3.5 Parametric Study

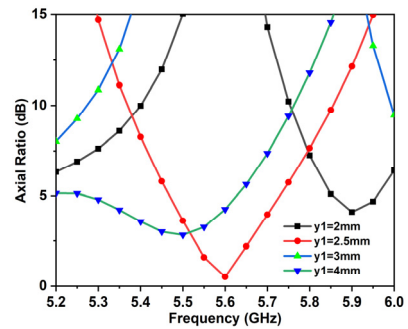
The parametric study is carried out and the results are depicted in Fig. 12. The position x_1 (starting position of the thin rectangular strip part of the unit cell) is varied in the positive x -direction and the respective S_{11} and axial ratio curves are plotted, and it is observed that at an optimum position of $x_1 = 5.5$ mm, the dual band nature with an axial ratio of less than 3 dB is achieved. It is also observed that without a significant degradation in the S_{11} performance of the antenna the CP is observed at this position. Since the narrow strip connecting the ground plane with the unit cell placed at the ground side aids the current flow, the starting position of the strip y_1 is varied along the positive y -direction and the respective S_{11} and axial ratio plots are indicated in Fig. 12(c) and (d). At an optimum position of $y_1 = 2.5$ mm, the restoration of dual band nature with CP in the second band is observed. The parametric analysis is conducted by keeping all the other parameters unchanged except the parameter under consideration.

Ref. No	No. of bands	Frequency (GHz)	Physical size (mm)	Electrical size	Impedance bandwidth (%)	Efficiency (%)	Gain (dBi)
[1]	2	2.46 5.5	36 × 24 × 1.59	0.26 × 0.19	3.65 52	64 89.2	0.71 1.53
[10]	2	2.5 5.8	44 × 70 × 1.6	0.36 × 0.58	22.8 10.8	94 92.1	> 0.2 > 3.1
[13]	2	1.8 5.2	40 × 36 × 1.6	0.24 × 0.21	2.2 13	>60	-2 4
[14]	2	2.45 5.5	38.2 × 29.1 × 6	0.31 × 0.23	4 12	84.2 90.3	2.3 8.6
[16]	2	2.76 5.23	36 × 36 × 3	0.33 × 0.33	1.44 3.05	79.4 90.8	1.02 6.8
[18]	2	2.6 3.6	31.7 × 27 × 1.6	0.27 × 0.23	2.2 28.53	79.3 95.6	<1.44 <1.98
[5]	3	2.45 3.5 4.7	32 × 25 × 0.064	0.26 × 0.2	6.1 18.2 27	-	2.1 2.8 3.5
[23]	3	1.78 4.22 5.8	20 × 20 × 0.508	0.11 × 0.11	3.08 15.17 8.33	70 96 >80	-0.15 2.18 3.58
[24]	3	2.6 3.6 5.8	35 × 32 × 1.6	0.3 × 0.27	7.7 14.1 10.7	-	0 1.6 2.7
Prop.	2	3.5 5.5	24 × 17 × 1.6	0.28 × 0.2	26.8 8.9	>82 >89	>2.9 >4.1

Tab. 2. Comparison of the proposed work with the existing literature.

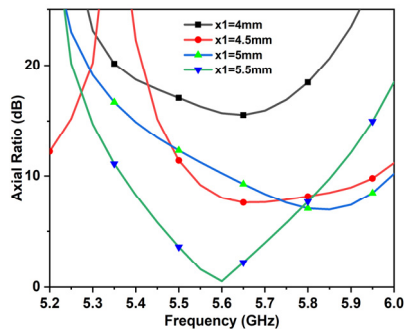


(a)

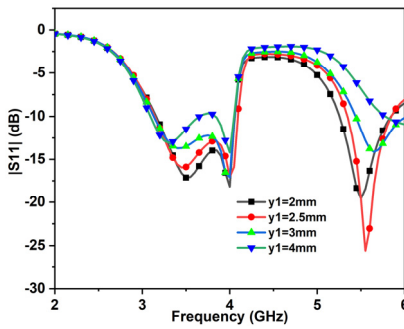


(d)

Fig. 12. Influence of variation in the position of the (a) x_1 on S_{11} , (b) x_1 on axial ratio, (c) y_1 on S_{11} , (d) y_1 on axial ratio.



(b)



(c)

The performance of several dual and tri band antennas that are composed of different metamaterial structures and operating in the similar frequency range which are published in the literature, are compared with the proposed antenna in Tab. 2. It can be summarized that the designed antenna offers a larger fractional bandwidth over the first band when compared with other literature mentioned in the table and the antenna also offers circular polarization in the second band with a considerably smaller size. Moreover, the antenna offers a better average gain across both the bands with good radiation efficiencies throughout the bands. Hence the antenna can become a good candidate for several Wi-Fi applications.

4. Conclusion

A new compact CRLH MTM-TL based dual band antenna for wireless applications has been proposed. It makes use of a low cost FR4 substrate with a planar struc-

ture and hence can be easily fabricated. The CRLH MTM inspired unit cell composed of inductors and capacitors induce the dual band nature with center frequencies of 3.5 GHz and 5.5 GHz. The percentage impedance bandwidths of the antenna in the two bands are 26.8 and 8.9 with the peak gains ranging in-between 2.9–4 dBi and 4.1–5.2 dBi. The antenna is linearly polarized in the first band and circularly polarized in the second with good radiation characteristics. A decent size reduction is achieved with a good matching between the simulated and measured results. The antenna has a great potential to be installed in 3.5/5.5 WiMAX bands and the sub-6 GHz 5G bands.

References

- [1] ZHU, J., ELEFThERIADES, G. V. Dual-band metamaterial-inspired small monopole antenna for WiFi applications. *Electronics Letters*, 2009, vol. 45, no. 22, p. 1104–1106. DOI: 10.1049/el.2009.2107
- [2] GHAFAR, A., AWAN, W. A., HUSSAIN, N., et al. A compact dual-band flexible antenna for applications at 900 and 2450 MHz. *Progress In Electromagnetics Research Letters*, 2021, vol. 99, p. 83–92. DOI: 10.2528/PIERL21060601
- [3] HERRAIZ-MARTINEZ, F. J., ZAMORA, G., PAREDES, F., et al. Multiband printed monopole antennas loaded with OCSRRs for PANs and WLANs. *IEEE Antennas and Wireless Propagation Letters*, 2011, vol. 10, p. 1528–1531. DOI: 10.1109/LAWP.2011.2181309
- [4] AWAN, W. A., GHAFAR, A., HUSSAIN, N., et al. CPW-fed dual-band antenna for 2.45/5.8 GHz applications. In *8th IEEE Asia-Pacific Conference on Antennas and Propagation (APCAP)*. Incheon (South Korea), 2019, p. 246–247. DOI: 10.1109/APCAP47827.2019.9471961
- [5] ZAIDI, A., AWAN, W. A., HUSSAIN, N., et al. A wide and tri-band flexible antennas with independently controllable notch bands for Sub-6-GHz communication system. *Radioengineering*, 2020, vol. 29, no. 1, p. 44–51. DOI: 10.13164/re.2020.0044
- [6] LI, H., ZHENG, Q., DING, J., et al. Dual-band planar antenna loaded with CRLH unit cell for WLAN/WiMAX application. *IET Microwaves, Antennas & Propagation*, 2018, vol. 12, no. 1, p. 132–136. DOI: 10.1049/iet-map.2016.1133
- [7] GHAFAR, A., LI, X. J., AWAN, W. A., et al. Design and realization of a frequency reconfigurable multimode antenna for ISM, 5G-Sub-6-GHz, and S-band applications. *Applied Sciences*, 2021, vol. 11, no. 4, p. 1–14. DOI: 10.3390/app11041635
- [8] BORHANI, M., REZAEI, P., VALIZADE, A. Design of a reconfigurable miniaturized microstrip antenna for switchable multiband systems. *IEEE Antennas and Wireless Propagation Letters*, 2015, vol. 15, p. 822–825. DOI: 10.1109/LAWP.2015.2476363
- [9] GHAFAR, A., LI, X. J., AWAN, W. A., et al. Capacitor loaded dual-band flexible antenna for ISM band applications. In *9th IEEE Asia-Pacific Conference on Antennas and Propagation (APCAP)*. Xiamen (China), 2020, p. 1–2. DOI: 10.1109/APCAP50217.2020.9246091
- [10] CHIEN, H. Y., SIM, C. Y. D., LEE, C. H. Dual-band meander monopole antenna for WLAN operation in laptop computer. *IEEE Antennas and Wireless Propagation Letters*, 2013, vol. 12, p. 694–697. DOI: 10.1109/LAWP.2013.2263373
- [11] SONAK, R., AMEEN, M., CHAUDHARY, R. K. CPW-fed electrically small open-ended zeroth order resonating metamaterial antenna with dual-band features for GPS/WiMAX/WLAN applications. *AEU-International Journal of Electronics and Communications*, 2019, vol. 104, p. 99–107. DOI: 10.1016/j.aeue.2019.03.017
- [12] ZARRABI, F. B., AHMADIAN, R., RAHIMI, M., et al. Dual band antenna designing with composite right/left-handed. *Microwave and Optical Technology Letters*, 2015, vol. 57, no. 4, p. 774–779. DOI: 10.1002/mop.28960
- [13] TAMRAKAR, M., KOMMURI, U. K. Dual band CRLH metal antenna for WLAN applications. *Wireless Personal Communications*, 2021, vol. 116, no. 4, p. 3235–3246. DOI: 10.1007/s11277-020-07846-6
- [14] AMEEN, M., MISHRA, A., CHAUDHARY, R. K. Dual-band CRLH-TL inspired antenna loaded with metasurface for airborne applications. *Microwave and Optical Technology Letters*, 2021, vol. 63, no. 4, p. 1249–1256. DOI: 10.1002/mop.32725
- [15] ZONG, B., WANG, G., ZHO, C., et al. Compact low-profile dual-band patch antenna using novel TL-MTM structures. *IEEE Antennas and Wireless Propagation Letters*, 2014, vol. 14, p. 567–570. DOI: 10.1109/LAWP.2014.2372093
- [16] MAJEDI, M. S., ATTARI, A. R. Dual-band resonance antennas using epsilon negative transmission line. *IET Microwaves, Antennas & Propagation*, 2013, vol. 7, no. 4, p. 259–267. DOI: 10.1049/iet-map.2012.0542
- [17] SI, L. M., ZHU, W., SUN, H. J. A compact, planar, and CPW-fed metamaterial-inspired dual-band antenna. *IEEE Antennas and Wireless Propagation Letters*, 2013, vol. 12, p. 305–308. DOI: 10.1109/LAWP.2013.2249037
- [18] PIROOJ, A., NASER-MOGHADASI, M., ZARRABI, F. B. Design of compact slot antenna based on split ring resonator for 2.45/5 GHz WLAN applications with circular polarization. *Microwave and Optical Technology Letters*, 2016, vol. 58, no. 1, p. 12–16. DOI: 10.1002/mop.29484
- [19] ZHOU, C., WANG, G., WANG, Y., et al. CPW-fed dual-band linearly and circularly polarized antenna employing novel composite right/left-handed transmission-line. *IEEE Antennas and Wireless Propagation Letters*, 2013, vol. 12, p. 1073–1076. DOI: 10.1109/LAWP.2013.2279689
- [20] HUSSAIN, N., NAQVI, S. I., AWAN, W. A., et al. A metasurface-based wideband bidirectional same-sense circularly polarized antenna. *International Journal of RF and Microwave Computer-Aided Engineering*, 2020, vol. 30, no. 8, p. 1–10. DOI: 10.1002/mmce.22262
- [21] HUSSAIN, N., JEONG, M. J., PARK, I., et al. A broadband circularly polarized Fabry-Perot resonant antenna using a single-layered PRS for 5G MIMO applications. *IEEE Access*, 2019, vol. 7, p. 42897–42907. DOI: 10.1109/ACCESS.2019.2908441
- [22] HUSSAIN, N., PARK, I. Design of a wide-gain-bandwidth metasurface antenna at terahertz frequency. *AIP Advances*, 2017, vol. 7, no. 5, p. 1–11. DOI: 10.1063/1.4984274
- [23] AMANI, N., KAMYAB, M., JAFARGHOLI, A., et al. Compact tri-band metamaterial-inspired antenna based on CRLH resonant structures. *Electronics Letters*, 2014, vol. 50, no. 12, p. 847–848. DOI: 10.1049/el.2014.0875
- [24] SAURAV, K., SARKAR, D., SRIVASTAVA, K. V. CRLH unit-cell loaded multiband printed dipole antenna. *IEEE Antennas and Wireless Propagation Letters*, 2014, vol. 13, p. 852–855. DOI: 10.1109/LAWP.2014.2320918
- [25] HUANG, H., LIU, Y., ZHANG, S., et al. Multiband metamaterial-loaded monopole antenna for WLAN/WiMAX applications. *IEEE Antennas and Wireless Propagation Letters*, 2014, vol. 14, p. 662–665. DOI: 10.1109/LAWP.2014.2376969
- [26] ABDALLA, M. A., HU, Z., MUVIANTO, C. Analysis and design of a triple band metamaterial simplified CRLH cells loaded

monopole antenna. *International Journal of Microwave and Wireless Technologies*, 2017, vol. 9, no. 4, p. 903–913. DOI: 10.1017/S1759078716000738

About the Authors ...

Junuthula ASHISH received his master's degree from the National Institute of Technology, Warangal, India in 2017. He is currently with Electronics and Communication Department, working towards his Ph.D. at the National Institute of Technology, Warangal, India. His research interests include multiband antennas, metamaterial antennas and reconfigurable antennas.

Amara PRAKASA RAO obtained his bachelor's degree in ECE from Nagarjuna University, A.P., India, and a master's degree from PEC-Pondicherry, India, with Electronics and Communication Engineering as specialization in 1994 and 1998. His doctoral degree is from the National Institute of Technology Warangal, India, in the year 2018. He has more than 20 years of experience in teaching at various organizations. Currently, he is with the Department of Electronics and Communication Engineering as an Associate Professor at the National Institute of Technology, Warangal, India. About 20 papers are at his credit in international and national journals and conferences. His areas of interest include signal processing, smart antenna systems, and optimization techniques.